


Article

Parameter Optimization and Effect Analysis of Low-Pressure Abrasive Water Jet (LPAWJ) for Paint Removal of Remanufacturing Cleaning

Sheng Xiong ^{1,2}, Xiujie Jia ^{1,2,*} , Shuangshuang Wu ^{1,2}, Fangyi Li ^{1,2}, Mingliang Ma ^{1,2} and Xing Wang ^{1,2}

¹ Key Laboratory of High Efficiency and Clean Mechanical Manufacture, Ministry of Education, School of Mechanical Engineering, Shandong University, Jinan 250061, China; xiongsheng2012ustb@163.com (S.X.); 18332722085@163.com (S.W.); lifangyi@sdu.edu.cn (F.L.); mingliang_ma@163.com (M.M.); wx1262812261@163.com (X.W.)

² National Demonstration Center for Experimental Mechanical Engineering Education, Shandong University, Jinan 250061, China

* Correspondence: xjjia@sdu.edu.cn

Abstract: As an environmentally friendly method, water jet (WJ) technology plays a significant role in the field of remanufacturing cleaning. The cleaning capacity of a WJ is severely restricted by the water pressure, while the impact force will be too large and may damage the cleaned substrate as well as cause energy waste if the pressure is too high. However, by adding abrasives, the cleaning capacity of a low-pressure water jet (LPWJ) will be considerably improved. Although abrasive water jet (AWJ) technology has been used in mechanical machining for decades, very limited research work can be found in the literature for remanufacturing cleaning. In this paper, the role of abrasives in low-pressure abrasive water jet (LPAWJ) cleaning was described. Cleaning performance with different parameters (abrasive feed rate condition, water pressure and standoff distance) in paint removal was experimentally investigated by using the Taguchi design of experiment. The experimental results indicated that the water pressure was the most dominant factor and the optimal parameter combination was the second feed rate condition, 9 MPa water pressure and 300 mm standoff distance. The influence law between the cleaning performance and various factors was explored, which can provide remanufacturers with directions in selection of the optimal parameters in the LPAWJ cleaning process. By designing contrast experiments, the results showed that the cleaning capacity of an LPAWJ is better than that of a pure LPWJ and the residual effect in terms of changes in surface roughness, residual stress and morphology is a little larger.

Keywords: low-pressure abrasive water jet (LPAWJ) cleaning; remanufacturing; paint removal; Taguchi method; cleaning rate; surface roughness; surface residual stress



Citation: Xiong, S.; Jia, X.; Wu, S.; Li, F.; Ma, M.; Wang, X. Parameter Optimization and Effect Analysis of Low-Pressure Abrasive Water Jet (LPAWJ) for Paint Removal of Remanufacturing Cleaning. *Sustainability* **2021**, *13*, 2900. <https://doi.org/10.3390/su13052900>

Academic Editor: Chunjiang An

Received: 27 January 2021

Accepted: 1 March 2021

Published: 8 March 2021

Publisher's Note: MDPI stays neutral with regard to jurisdictional claims in published maps and institutional affiliations.



Copyright: © 2021 by the authors. Licensee MDPI, Basel, Switzerland. This article is an open access article distributed under the terms and conditions of the Creative Commons Attribution (CC BY) license (<https://creativecommons.org/licenses/by/4.0/>).

1. Introduction

Large amounts of end-of-life products scrapped directly have led to excessive waste of resources over recent years, which can be significantly improved by remanufacturing [1–3]. Remanufacturing is an industrial process whereby used products can be restored to useful life [4], including design [5], disassembly [6], cleaning [7], inspection [8], reconditioning [9], etc., among which cleaning is a particularly essential procedure because the cleanliness of cleaned substrate has a significant influence on the following procedures. The ideal state of remanufacturing cleaning is to remove all the contaminants on the surface without affecting the substrate [10]. The components of the surface contaminants are complicated, mainly including dust, sludge, rust, carbon deposition, paint, etc., among which paint is the closest layer to the substrate, which makes paint removal in condition of having as little effect on the substrate as possible a significant problem [11].

Various cleaning technologies have been used in many countries to remove paint, such as water jet (WJ) cleaning [12], laser cleaning [13], molten salt cleaning [14,15], su-

percritical carbon dioxide cleaning [16,17] and dry abrasive blasting cleaning [18,19]. As an improved alternative to conventional WJ cleaning technology, abrasive water jet (AWJ) cleaning technology has been receiving more and more attention, especially in the area of remanufacturing.

In an AWJ cleaning system, the cleaning capacity of a mixed jet is affected by many parameters, including abrasives (type, particle size and feed rate condition) [20,21], injection (angle, distance, pressure and cleaning time) [22], nozzle (material and structure) [23], etc. Three among these are dominant process parameters: abrasive feed rate condition, water pressure and standoff distance. When the abrasive concentration increases, the overall energy transfer rate from water to the abrasive can be considerably improved [24]. Furthermore, both inlet water pressure and standoff distance can influence the velocity and pressure distribution of a jet significantly [12]. However, most previous studies mainly focused on the machining and cutting capacity of AWJs [25–28], whereas knowledge is still limited about the cleaning performance. Additionally, in order to decrease the impact on the substrate, the water pressure used for cleaning was less than 10 MPa, which may reach dozens to hundreds MPa when used in the machining field [29,30].

In this study, the mass flow of abrasives under different water pressure and feed rate conditions was measured using an overall experiment method. A Taguchi orthogonal experiment was designed to explore the influence law of abrasive feed rate condition, water pressure and standoff distance on the cleaning capacity of a low-pressure abrasive water jet (LPAWJ). The study findings provide important information on the different contributions of these three factors in an LPAWJ system and can help remanufacturers to select the optimal parameters in the cleaning process. Besides, through surface roughness and residual stress measurement as well as morphology observation [31], the effect on the cleaned substrate after LPAWJ cleaning was analyzed and compared with pure LPWJ cleaning.

2. Equipment, Materials and Methods

2.1. Equipment

Figure 1 shows the photograph and the schematic diagram of the experiment equipment (main parameters are shown in Table 1), which was constructed at the Shandong University (SDU) to simulate the enclosed cleaning operations. Water was compressed by a plunger pump (EL1713, Interpump, Reggio nell'Emilia, Italy) and then formed a jet in the mixing chamber through a WJ nozzle. In this process, abrasives entered into the WJ by the joint force of their gravity and the negative pressure generated by the WJ in the mixing chamber. Finally, through the nozzle, the AWJ mixed by water and abrasives was formed. Abrasive feed rate condition could be adjusted from level 0 to 3 (0 means closed, 3 means fully open) by rotating the control valve to increase the mass flow rate of abrasives. The specific value of mass flow rate of abrasives is discussed in Section 2.3, which was influenced both by abrasive feed rate and water pressure. The work piece to be cleaned was clamped on the worktable, of which the position could be altered by a lead-screw nut mechanism. In addition, the water and abrasives used in this cleaning process can be recycled and reused by setting the filter device [32]. In order to avoid flash rust appearing on the substrate, rust inhibitor was added into the water system. After cleaning, specimens were dried by a hot air blower as soon as possible, and then, photos of the cleaned specimens were taken by camera. Surface morphology observation and roughness measurements were carried out using an optical profiler (NT9300, WYKO, Greenback, TN, USA). The measurement window size was $640 \times 480 \mu\text{m}$ without filtering setting and the final roughness R_a value was the average of 5 measurements (one central measuring point and four surrounding measuring points randomly selected in the cleaned area). Residual stress on the cleaned surface was measured using an X-ray stress analyzer (XSTRESS3000, AST-STRESSTECH, Finland).

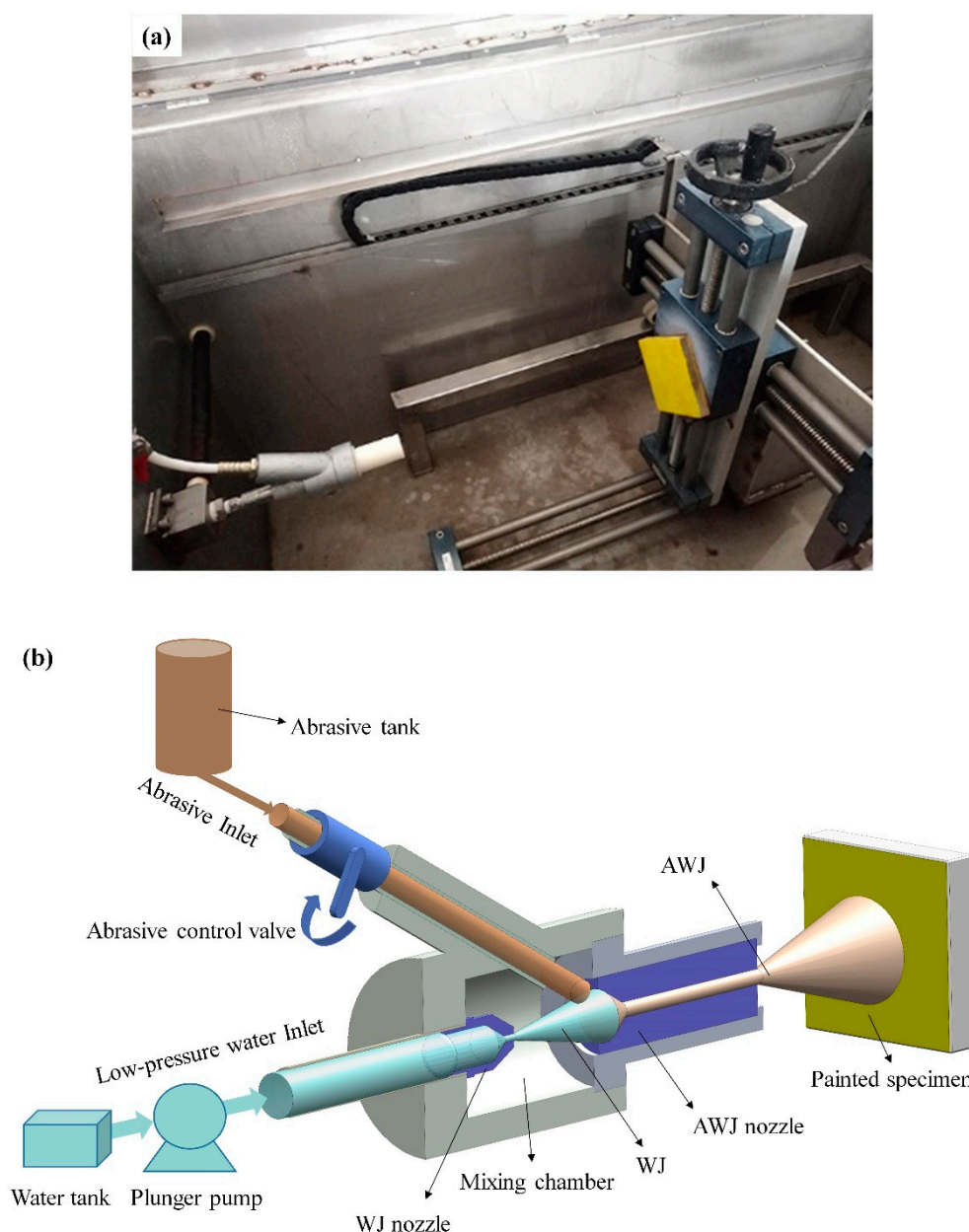


Figure 1. (a) The low-pressure abrasive water jet (LPAWJ) cleaning equipment; (b) schematic diagram.

Table 1. Main parameters of the equipment.

Main Parameters	Values or Materials
Maximum pump pressure	17 MPa
Maximum water flow rate	13 L·min ^{−1}
Maximum standoff distance	500 mm
Abrasive feed rate condition	0,1,2,3
Maximum abrasive mass flow rate	360 kg·h ^{−1}
WJ nozzle material	SUS 316 L
WJ nozzle diameter	φ1.8 mm
AWJ nozzle material	Boron carbide
AWJ nozzle diameter	φ4 mm
AWJ nozzle length	60 mm
Mixing chamber diameter	φ36 mm
Mixing chamber length	50 mm

2.2. Materials

Considering that the surface shape of parts recycled for remanufacturing is usually curved, such as a valve stem, sleeve and so on, which makes it difficult to obtain flat and uniform samples with enough area for experiments, specimens were chosen, instead, to study the influence law of different parameters in the cleaning process. Specimens were Q345C steel substrates (frequently used material of engineering parts) of size $50 \times 50 \times 10 \text{ mm}^3$, artificially coated with acrylic polyurethane paint. In order to guarantee the identity of surfaces before spray paints, the steels were polished by sandpapers ranging from 400# to 1200# and then cleaned by ultrasonic cleaning in an anhydrous alcohol medium. Through measurement, the surface roughness Ra value and residual stress of untreated samples were $1.63 \text{ }\mu\text{m}$ and -30.1 MPa , respectively. The paint thickness of each spray was 0.02 mm and the final thickness was 0.1 mm by spraying 5 times with a 20-min time interval between 2 sprays. After spraying, the specimens were naturally dried for 1 month to mimic the actual coatings on remanufacturing parts.

In order to obtain satisfactory cleaning capacity and minor surface damage, 80# white corundum (particle size about $180 \text{ }\mu\text{m}$, mainly Al_2O_3 99.0% and others; material properties are shown in Table 2) was chosen as the cleaning abrasive, which only has a small effect on the substrate because of its small size and will not cause iron element pollution on the cleaned substrate because of its extremely low element content of Fe.

Table 2. Material properties of 80# white corundum.

Bulk Density ($\text{kg}\cdot\text{m}^{-3}$)	Specific Gravity	Mohs Hardness
2.53×10^3	2.5	9

2.3. Calculation of Cleaning Rate and Abrasive Mass Flow Rate

To appraise the cleaning capacity of the jets with different combinations of parameters, the values of cleaning rate were calculated after experiment. As the weight of paint is very light when compared with the specimen, which makes it quite difficult to measure the paint weight loss during cleaning process, the image method was chosen to calculate the cleaning rate, which is the area ratio of the cleaned surface to the entire surface. The concrete steps of the image method are as follows:

1. Crop the photo taken after cleaning and delete the treated area from the specimen;
2. Convert the color of the cleaned area to white and that of the paint to black using the graphic processing software Adobe Photoshop CC;
3. Calculate the ratio of the number of white pixels to the total pixels using MATLAB version R2018b software through the code shown in Appendix A.

The cleaning rate was calculated using the following formula:

$$R = \frac{A_C}{A_T} = \frac{N_C}{N_T}, \quad (1)$$

where R is the cleaning rate; A_C and A_T are the areas of the cleaned surface and the total surface, respectively; N_C and N_T are the numbers of the white pixels and the total pixels, respectively.

In order to obtain the mass flow of abrasives during the cleaning process, the abrasive tank used was cylindrical with a scale inside. The volume of abrasives consumed can be calculated by reading the drop value on the scale and the mass flow rate of the abrasive can be determined using the following equation:

$$F = \frac{\rho \pi r^2 (h_1 - h_2)}{t}, \quad (2)$$

where F ($\text{kg}\cdot\text{h}^{-1}$) is the mass flow of the abrasive; ρ ($\text{kg}\cdot\text{m}^{-3}$) is the bulk density of 80# white corundum; r (m) is the radius of the abrasive tank; h_1 and h_2 (m) are the scale

readings in the abrasive tank before and after the cleaning process, respectively; t (h) is the cleaning time.

By adjusting the abrasive feed rate condition and water pressure, the mass flow rate of abrasive was measured and calculated as shown in Table 3. When the abrasive feed rate condition was set as 0 (closing the abrasive control valve), this equipment could realize pure water jet cleaning.

Table 3. Abrasive mass flow rate under different parameters.

Abrasive Feed Rate Condition	Water Pressure (MPa)	Abrasive Mass Flow Rate ($\text{kg}\cdot\text{h}^{-1}$)
0	* 1	0
1	5	41.08
1	7	64.73
1	9	125.77
2	5	90.11
2	7	129.29
2	9	168.10
3	5	167.67
3	7	185.54
3	9	210.98

* 1 No data needs to be filled in here.

Figure 2 shows that the mass flow rate of abrasives increased along with both the water pressure and the abrasive feed rate condition.

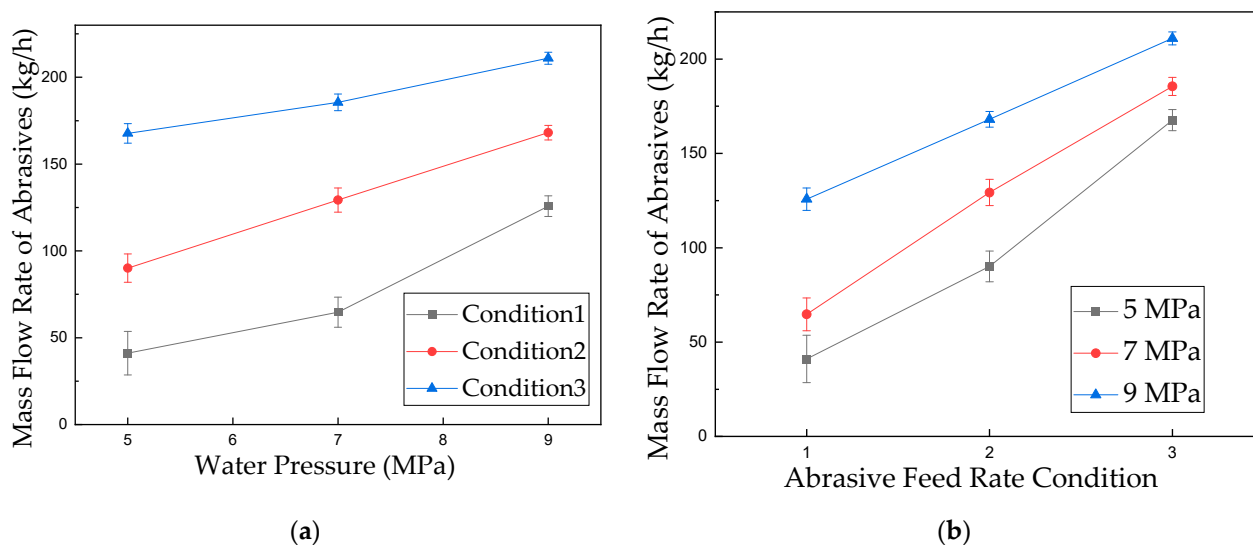


Figure 2. The relationship between the mass flow rate of abrasives and different factors: (a) Water pressure; (b) abrasive feed rate condition.

The maximum mass flow rate was $210.98 \text{ kg}\cdot\text{h}^{-1}$ with the third feed rate condition and 9 MPa water pressure, while the minimum value was $41.08 \text{ kg}\cdot\text{h}^{-1}$ with the first feed rate condition and 5 MPa water pressure. When the abrasive feed rate condition was fixed, the mass flow increased with the increase in water pressure. Similarly, when the water pressure was fixed, the mass flow increased with the increase in abrasive feed rate condition. This trend may result from the following reasons:

With the increment in abrasive feed rate, the channel from the abrasive tank to the mixing chamber becomes larger; thus, the number of abrasives entering into mixing chamber will increase. As for the water pressure, the suction force produced by negative pressure surrounding the water jet will increase with the increase in pressure, which also contributes to the improvement of mass flow of abrasives.

2.4. Design of Experiment and Statistical Analysis

Designing of the cleaning experiment and statistical analysis were performed using Minitab version 16 software. The cleaning experiments were designed using the Taguchi orthogonal method, which can obtain the influence law and significance level of each parameter on the cleaning effect accurately and efficiently. As shown in Table 4, abrasive feed rate condition, water pressure (MPa) and standoff distance (mm) were selected as factors at three levels. The cleaning time was set as 10 s, which can reflect the difference of various factors' combination according to the previous test results. In order to completely demonstrate the cleaning capacity of the jet and the effect caused on the substrate, the position of the specimen was fixed during the cleaning process and the injection angle was set as 90 degrees.

Table 4. Parameters with respective levels.

Parameters	Level 1	Level 2	Level 3
Abrasive feed rate condition	1	2	3
Water pressure (MPa)	5	7	9
Standoff distance (mm)	200	300	400

Table 5 presents the L₉ orthogonal design array of the experiments as well as the cleaning results including cleaning rate, values of surface roughness *Ra* and residual stress. After the experiments, the data were evaluated using the range method and analysis of variance (ANOVA). Significant differences were accepted at the 0.05 level.

Table 5. Design of Taguchi experiments and the results.

Experiments	Abrasive Feed Rate Condition	Water Pressure (MPa)	Standoff Distance (mm)	Cleaning Rate (%)	Surface Roughness <i>Ra</i> (μm)	Surface Residual Stress (MPa)
1	1	5	200	0.06	4.38	−83.2
2	1	7	300	12.72	2.02	−157.7
3	1	9	400	24.19	2.91	−150.7
4	2	5	300	13.57	2.34	−136.6
5	2	7	400	15.58	2.22	−155.7
6	2	9	200	27.30	2.33	−138.4
7	3	5	400	≈0 ¹	3.06	−36.6
8	3	7	200	6.56	2.48	−143.6
9	3	9	300	26.47	2.49	−143.1

¹ Only very little paint had been removed.

3. Results and Discussion

3.1. Comparison of Cleaning Capacity between LPWJ and LPAWJ

As shown in Figure 3, in order to compare the different cleaning capacities of LPWJ and LPAWJ, controlled experiments were performed under the condition of 9 MPa water pressure and 300 mm standoff distance. In the LPAWJ cleaning experiment, the abrasive feed rate condition was set at the second level (abrasive mass flow rate was about 168.10 kg·h^{−1}), which was the only different parameter between the two controlled experiments.

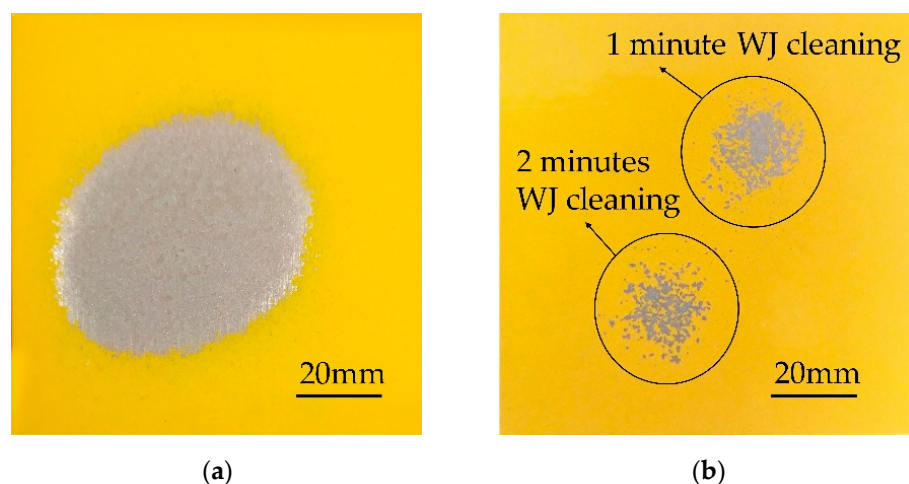


Figure 3. Specimens cleaned by different cleaning methods: (a) LPAWJ cleaning of 10 s; (b) low-pressure water jet (LPWJ) cleaning of 1 min and 2 min.

When the accelerated abrasives impacted the specimen, the paint on the substrate was extruded at first, then ploughed by the interfacial shear stress generated in the collision and, finally, removed by the continuous flow of abrasives [33].

3.2. Range Analysis and ANOVA of Cleaning Rate

As shown in Figure 4 and Table 5, the cleaning rates of the first and seventh experiments were 0.06% and nearly 0%, respectively, which were quite small when compared with the other values. The results indicated that the LPAWJ under these two combinations of factors can hardly remove paint. Therefore, it can be concluded that there exists a threshold of cleaning capacity of the LPAWJ during the process of paint removal. When the cleaning capacity is weaker than the threshold, the impact of the jet is too light to remove the paint, while the cleaning efficiency will be significantly improved if the cleaning capacity is greater than the threshold.

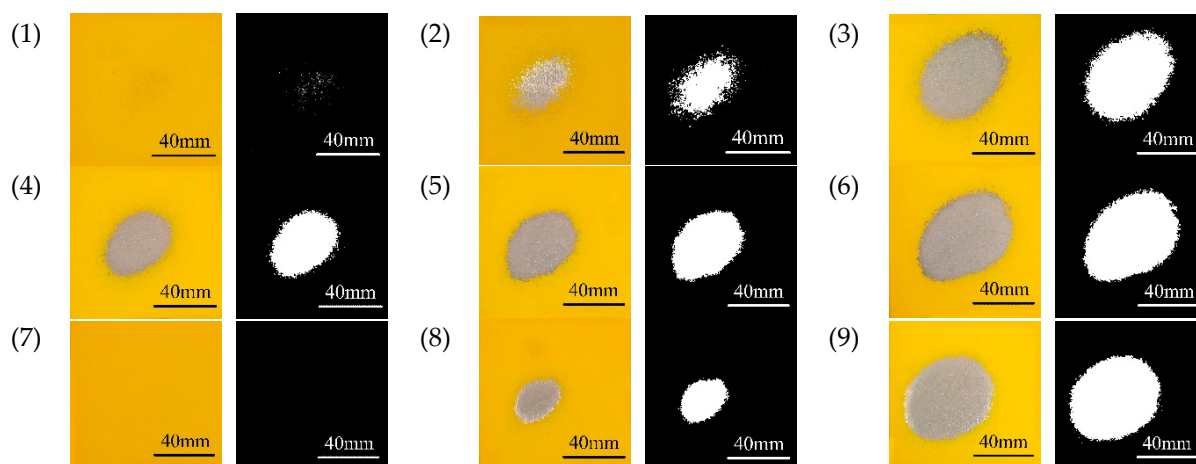


Figure 4. Photos of specimens after cropping and converting.

The range analysis results of cleaning rate can be observed in Table 6, where the maximum and minimum values of range were 21.44 for water pressure and 6.28 for standoff distance, respectively, which meant that water pressure had the biggest contribution to cleaning capacity while standoff distance had the smallest within the experimental scope. The rank results indicated that the cleaning factors affecting the cleaning rate are in the following order: water pressure > abrasive feed rate condition > standoff distance.

Table 6. Range analysis of cleaning rate.

Parameters	Level 1	Level 2	Level 3	Range	Rank
Abrasive feed rate condition	12.32	18.82	11.01	7.81	2
Water pressure (MPa)	4.54	11.62	25.99	21.44	1
Standoff distance (mm)	11.31	17.59	13.26	6.28	3

Additionally, in order to show the significance level of each factor, Table 7 presents the ANOVA results of the experimental data. The p values of water pressure, abrasive feed rate condition and standoff distance were 0.004, 0.029 and 0.047, respectively. All of the three p values were less than 0.05, meaning that all three parameters were significant. Furthermore, the sequencing of the three p values in numerical order from small to large was as same as the result of range method, which can also validate the accuracy of this experiment to some extent.

Table 7. ANOVA of cleaning rate.

Parameters	Degree of Freedom	Sum of Square	Variance	F Value	p Value
Abrasive feed rate condition	2	104.83	52.42	34.01	0.029
Water pressure (MPa)	2	716.30	358.15	232.38	0.004
Standoff distance (mm)	2	61.99	30.99	20.11	0.047
Residual	2	3.08	1.54	*	*
Total	8	886.20	*	*	*

Taking the levels of each parameter as the horizontal axis and the values of cleaning rate as the vertical axis, the main effect diagram of cleaning rate can be obtained as shown in Figure 5.

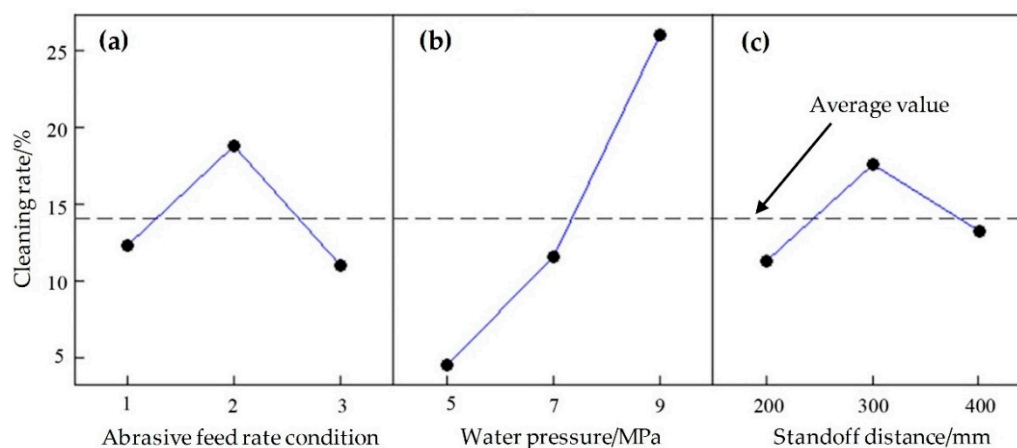


Figure 5. Main effect diagram of cleaning rate vs. different factors: (a) Abrasive feed rate condition; (b) water pressure; (c) standoff distance.

As shown in Figure 5b, with the increase in water pressure, the cleaning rate increased rapidly. The higher the water pressure, the stronger the acceleration effect of abrasives; thus, the impact force from jet to paint can be greater, which means a better cleaning capacity. Furthermore, as shown in Figure 2, the number of abrasives rose steadily along with water pressure, which can also contribute to the improvement of cleaning capacity.

However, too many abrasives in the cleaning jet may produce reverse effects on the cleaning capacity. With the increment in abrasive feed rate condition from levels 1 to 3, the cleaning rate first increased and then decreased as displayed in Figure 5a. Although the cleaning capacity of the jet can be enhanced due to the increase in abrasive mass fraction at the beginning, in the mixing chamber with limited volume, when more abrasives entered into the jet, more speed loss because of collision between abrasives would happen, which

can eventually lead to a reduction in cleaning capacity. In addition, the probability of collision between the abrasives first impacting and then rebounding from the coating surface and the latter coming ones would increase, which can also bring a negative effect in the cleaning process.

Besides, Figure 5c demonstrates that the trend of standoff distance on cleaning rate was the same as the abrasive feed rate condition, which indicated that an optimal distance in the cleaning system exists. This finding was consistent with previous studies using pure WJ cleaning experiments [12]. Before reaching the optimal value, with the extension of standoff distance, the range of the cleaned area will be enlarged; thus, the cleaning efficiency can be improved. Nevertheless, when the optimal distance is exceeded, the phenomenon of jet divergence and velocity attenuation cannot be negligible, which may decrease the overall cleaning capacity and be reflected in the downward trend of cleaning rate.

Finally, according to the analysis of these three factors above, it can be obtained that within the experimental scope, the optimal parameter combination was the second feed rate condition, 9 MPa water pressure and 300 mm standoff distance. However, this combination was not included in the Taguchi orthogonal experimental design. Therefore, two verification experiments were performed, and the average value of cleaning rate was 33.4%, which was greater than that of the previous nine groups, just as predicted. Besides, the average of surface roughness R_a value and residual stress was 2.87 μm and -154.8 MPa, respectively.

3.3. Analysis of Residual Effect on the Cleaned Surface

The damage effect on the cleaned substrate after cleaning can be analyzed and compared by surface roughness and residual stress measurements as well as surface morphology observation.

Values of the surface roughness R_a and residual stress under different treatments are shown in Table 8. In the controlled experiments, the surface roughness R_a value slightly increased after LPWJ cleaning. Although only little paint was removed, the surface residual compressive stress reached -129.2 MPa after 1 min of WJ cleaning and -147.3 MPa after 2 min, which meant that the LPWJ could have a significant influence on the surface residual stress after long-term impact, while the cleaning capacity was quite weak.

Table 8. Surface roughness R_a value and residual stress of specimens after different treatments.

	Before Painted	After Painted	1 min WJ Cleaning	2 min WJ Cleaning
Surface roughness R_a (μm)	1.63	0.38	1.81	2.06
Surface residual stress (MPa)	-30.1	*	-129.2	-147.3

In the Taguchi orthogonal experiments, as shown in Table 3, the roughness R_a values of the first and seventh experiments were 4.38 and 3.06 μm , respectively, while the other seven values were distributed from 2 to 3 μm without an obvious regular pattern through analysis using the range method and ANOVA (main effect diagram was irregular and all three p values were bigger than 0.05). These two unusually high values may result from their low cleaning rate, as mentioned above. Because, in this situation, the jet only removed a quite small amount of the paint layer on the surface, the area for roughness measurement was mixed by the remaining paint and cleaned substrate instead of pure cleaned substrate. The altitude difference between paint and substrate was relatively large, and therefore, these two abnormal values appeared. In order to obtain an accurate roughness R_a value, a chemical paint cleaning agent was used to remove the paint without affecting the substrate. Through measurement, the roughness R_a values of first and seventh experiments were found to be 1.89 and 1.65 μm , respectively. These two roughness values are very close to the measurement result of the untreated sample. Hence, it can be concluded that the effect of LPAWJ cleaning on the surface roughness is very small when only little paint is removed.

The average surface residual stress of the initial samples was -30.1 MPa, which may be introduced from the milling process. After LPAWJ cleaning, the residual compressive stress was increased to a greater or lesser extent. However, an obvious regular pattern of distribution of the measured data could not be discovered by the range method and ANOVA, as with the roughness Ra mentioned above. The residual stresses of the first and seventh experiments were -83.2 and -36.6 MPa, respectively, while the other seven stresses were distributed from -160 to -130 MPa. In the seventh experiment, only little paint had been removed, and the residual stress was very close to the untreated sample. However, with the increment in cleaning capacity, more paint was removed, and the residual stress reached -83.2 MPa in the first experiment. Without regard to these two exorbitant values of the first and seventh experiments, it can be concluded that the difference in residual stress effect on the cleaned surface under various factors' combination in LPAWJ cleaning is not significant within the experimental scope. In general, after LPAWJ cleaning, the surface residual compressive stress of the samples will be larger than the untreated one, which means a positive effect on the improvement of the material's fatigue life.

Figure 6 shows the morphology observations of the specimens' surfaces, tagged with the roughness Ra value.

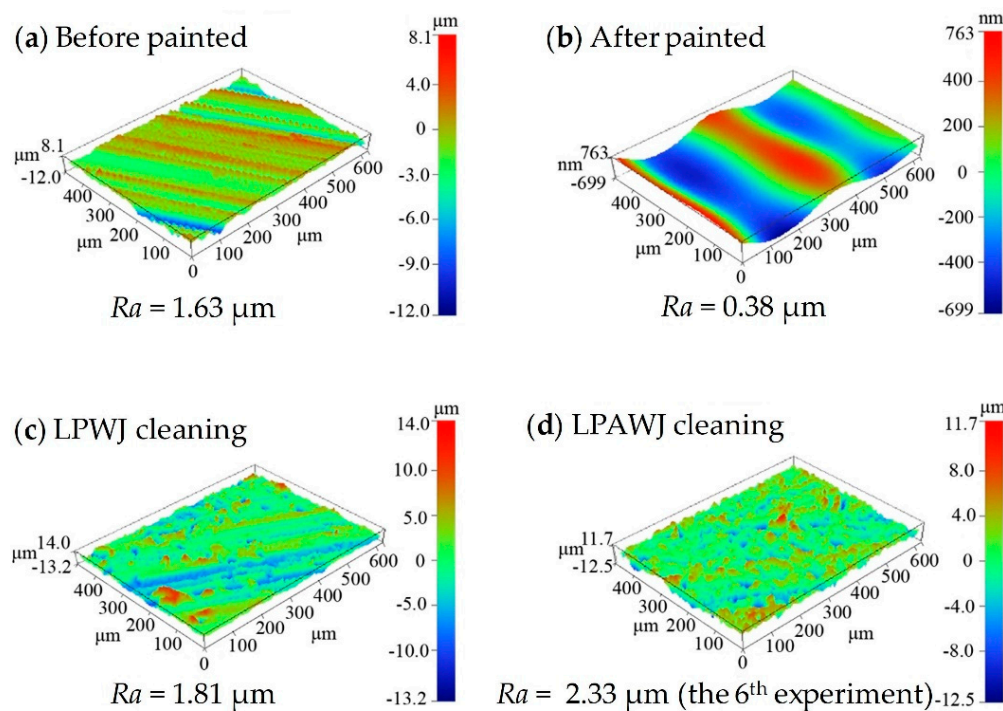


Figure 6. Surface morphology observations tagged with surface roughness Ra value of specimens after different treatments: (a) Before painted; (b) after painted; (c) LPWJ cleaning; (d) LPAWJ cleaning of sixth experiment.

The surface of the untreated sample presented the tool pattern left by the machining process and then covered by paint while the Ra value reduced from 1.63 to 0.38 μm . After pure LPWJ cleaning, the tool pattern could still be seen on the surface, and the Ra value slightly increased to 1.81 μm . However, the tool pattern was gone when LPAWJ cleaning was used, and the Ra value increased to about $2\sim3$ μm (the morphology observations were similar and the sixth experiment was chosen as a representative) under different cleaning parameters, while the surface shape of substrate became irregular with small bumps and pits appearing. The result indicated that LPAWJ usage for paint removal may produce a rougher surface when compared with LPWJ.

4. Conclusions

With few studies available on the contribution of water pressure, abrasive feed rate condition and standoff distance in paint removal for remanufacturing cleaning by LPAWJ cleaning, this study not only revealed the influence law of these three factors on the cleaning capacity of jets but also demonstrated the cleaning effect on the substrate after LPAWJ impacting and compared it with pure LPWJ cleaning. The main conclusions of this paper are drawn as follows:

1. The mass flow rate of abrasives increases along with both water pressure and abrasive feed rate condition.
2. There is a threshold of the cleaning capacity of LPAWJ cleaning. When the cleaning capacity is lower than the threshold, the jet can hardly remove the paint on the substrate, while the cleaning efficiency will be significantly improved when the cleaning capacity is greater than the threshold.
3. When using LPAWJ technology to clean paint, abrasives play the main role in paint removal, while water can accelerate abrasives.
4. Within the experimental scope, the optimal parameter combination was the second feed rate condition, 9 MPa water pressure and 300 mm standoff distance, and the corresponding cleaning rate, surface roughness R_a value and residual stress were 33.4%, 2.87 μm and -154.8 MPa, respectively.
5. The cleaning capacity of the jet increases obviously with the increase in water pressure, first increasing and then decreasing along with the abrasive feed rate condition and standoff distance within the experimental scope. The parameters affecting the cleaning capacity are in the following order: water pressure > abrasive feed rate condition > standoff distance.
6. The cleaning capacity of LPAWJ cleaning is better than pure LPWJ cleaning and the residual effect is a little larger within the experimental scope.

In order to analyze the cleaning capacity of water jets more accurately and efficiently, this study used a single area cleaning pattern without moving the specimens during the cleaning process, whereas a whole contaminated surface instead of one area needs to be cleaned in real remanufacturing factories. Therefore, more intensive studies will be carried out in the future, such as moving the samples while cleaning, changing the impact angle of LPAWJ, using various kinds of abrasives, etc.

Author Contributions: Conceptualization, S.X. and X.J.; methodology, S.X. and S.W.; software, S.X. and M.M.; validation, S.X. and X.W.; formal analysis, S.X.; investigation, S.X. and X.W.; resources, S.X. and S.W.; data curation, S.X.; writing—original draft preparation, S.X.; writing—review and editing, X.J.; visualization, S.X.; supervision, X.J. and F.L.; project administration, X.J. and F.L.; funding acquisition, X.J. All authors have read and agreed to the published version of the manuscript.

Funding: This research was funded by the National Natural Science Foundation of China (NSFC) through grant number 51875324 and The Key Science and Technology Innovation Project of Shandong Province through grant number 2018CXGC0807.

Institutional Review Board Statement: Not applicable.

Informed Consent Statement: Not applicable.

Data Availability Statement: Not applicable.

Conflicts of Interest: The authors declare no conflict of interest.

Appendix A

The MATLAB program code to calculate the cleaning rate is shown as follows:

```
photo = imread('C:/CleaningRateCalcu/xx.jpg');    % open the converted photo
subplot(2,1,1);
imshow(photo);                                  % show the photo
subplot(2,1,2);
imhist(photo);                                  % show the color histogram
[l,w] = size(photo);                             % get the length and width of the photo
total_pixels = l*w;                              % calculate the number of total pixels
white_pixels = length(find(photo == 255));        % calculate the number of white pixels
cleaning_rate = white_pixels/total_pixels;        % calculate the cleaning rate
```

References

- Subramoniam, R.; Huisingh, D.; Chinnam, R.B. Remanufacturing for the automotive aftermarket-strategic factors: Literature review and future research needs. *J. Clean. Prod.* **2009**, *17*, 1163–1174. [\[CrossRef\]](#)
- Charnley, F.; Tiwari, D.; Hutabarat, W.; Moreno, M.; Okorie, O.; Tiwari, A. Simulation to enable a data-driven circular economy. *Sustainability* **2019**, *11*, 3379. [\[CrossRef\]](#)
- Bernard, S. Remanufacturing. *J. Environ. Econ. Manag.* **2011**, *62*, 337–351. [\[CrossRef\]](#)
- Seitz, M.A. A critical assessment of motives for product recovery: The case of engine remanufacturing. *J. Clean. Prod.* **2007**, *15*, 1147–1157. [\[CrossRef\]](#)
- Hatcher, G.D.; Ijomah, W.L.; Windmill, J.F.C. Design for remanufacture: A literature review and future research needs. *J. Clean. Prod.* **2011**, *19*, 2004–2014. [\[CrossRef\]](#)
- Meng, W.; Zhang, X. Optimization of remanufacturing disassembly line balance considering multiple failures and material hazards. *Sustainability* **2020**, *12*, 7318. [\[CrossRef\]](#)
- Peng, S.; Li, T.; Tang, Z.; Shi, J.; Zhang, H. Comparative life cycle assessment of remanufacturing cleaning technologies. *J. Clean. Prod.* **2016**, *137*, 475–489. [\[CrossRef\]](#)
- Zhu, Y.; Liang, Y.; Wei, S.; Wang, Y.; Wang, B. Ultrasonic testing system design for defect visualization of inhomogeneous multi-layered pipes. *SN Appl. Sci.* **2019**. [\[CrossRef\]](#)
- Zhang, K.; Li, D.; Gui, H.; Li, Z. An adaptive slicing algorithm for laser cladding remanufacturing of complex components. *Int. J. Adv. Manuf. Technol.* **2019**. [\[CrossRef\]](#)
- Fadeyi, J.A.; Monplaisir, L.; Aguwa, C. The integration of core cleaning and product serviceability into product modularization for the creation of an improved remanufacturing-product service system. *J. Clean. Prod.* **2017**, *159*, 446–455. [\[CrossRef\]](#)
- Li, M.Z.; Liu, W.W.; Qing, X.C.; Yu, Y.; Liu, L.H.; Tang, Z.J.; Wang, H.J.; Dong, Y.Z.; Zhang, H.C. Feasibility study of a new approach to removal of paint coatings in remanufacturing. *J. Mater. Process. Technol.* **2016**, *234*, 102–112. [\[CrossRef\]](#)
- Guha, A.; Barron, R.M.; Balachandar, R. An experimental and numerical study of water jet cleaning process. *J. Mater. Process. Technol.* **2011**, *211*, 610–618. [\[CrossRef\]](#)
- Ma, M.; Wang, L.; Li, J.; Jia, X.; Wang, X.; Ren, Y.; Zhou, Y. Investigation of the surface integrity of Q345 steel after Nd:YAG laser cleaning of oxidized mining parts. *Coatings* **2020**, *10*, 716. [\[CrossRef\]](#)
- Zhang, B.; Jia, X.; Li, F.; Sun, Y. Research on the Effect of Molten Salt Ultrasonic Composite Cleaning for Paint Removal. *ACS Omega* **2019**, *4*, 17072–17082. [\[CrossRef\]](#)
- Long, Y.; Li, J.; Timmer, D.H.; Jones, R.E.; Gonzalez, M.A. Modeling and optimization of the molten salt cleaning process. *J. Clean. Prod.* **2014**, *68*, 243–251. [\[CrossRef\]](#)
- Liu, W.W.; Zhang, B.; Li, Y.Z.; He, Y.M.; Zhang, H.C. An environmentally friendly approach for contaminants removal using supercritical CO₂ for remanufacturing industry. *Appl. Surf. Sci.* **2014**, *292*, 142–148. [\[CrossRef\]](#)
- Li, M.; Liu, W.; Short, T.; Qing, X.; Dong, Y.; He, Y.; Zhang, H.C. Pre-treatment of remanufacturing cleaning by use of supercritical CO₂ in comparison with thermal cleaning. *Clean Technol. Environ. Policy* **2015**, *17*, 1563–1572. [\[CrossRef\]](#)
- Raykowski, A.; Hader, M.; Maragno, B.; Spelt, J.K. Blast cleaning of gas turbine components deposit removal and substrate deformation. *Wear* **2001**, *249*, 126–131. [\[CrossRef\]](#)
- Kambham, K.; Sangameswaran, S.; Datar, S.R.; Kura, B. Copper slag: Optimization of productivity and consumption for cleaner production in dry abrasive blasting. *J. Clean. Prod.* **2007**, *15*, 465–473. [\[CrossRef\]](#)
- Rosenberg, B.; Yuan, L.; Fulmer, S. Ergonomics of abrasive blasting: A comparison of high pressure water and steel shot. *Appl. Ergon.* **2006**, *37*, 659–667. [\[CrossRef\]](#) [\[PubMed\]](#)
- Schnakovszky, C.; Herghelegiu, E.; Radu, C.; Cristea, I. The influence of the feed rate on the quality of surfaces processed by AWJ at high pressures. In *Advanced Materials Research*; Trans Tech Publications: Bäch, Switzerland, 2014.
- Yang, M.; Choi, J.; Lee, J.; Hur, N.; Kim, D. Wet blasting as a deburring process for aluminum. *J. Mater. Process. Technol.* **2014**, *214*, 524–530. [\[CrossRef\]](#)
- Zhong, Z.W.; Han, Z.Z. Performance comparison of four waterjet nozzles. *Mater. Manuf. Process.* **2003**, *18*, 965–978. [\[CrossRef\]](#)
- Yu, Y.; Sun, T.; Yuan, Y.; Gao, H.; Wang, X. Experimental investigation into the effect of abrasive process parameters on the cutting performance for abrasive waterjet technology: A case study. *Int. J. Adv. Manuf. Technol.* **2020**, *107*, 2757–2765. [\[CrossRef\]](#)

-
25. Hashish, M. A modeling study of metal cutting with abrasive waterjets. *J. Eng. Mater. Technol. Trans. ASME* **1984**. [[CrossRef](#)]
 26. Zaki, M.; Corre, C.; Kuszla, P.; Chinesta, F. Numerical simulation of the abrasive waterjet (AWJ) machining: Multi-fluid solver validation and material removal model presentation. *Int. J. Mater. Form.* **2008**. [[CrossRef](#)]
 27. Hlaváč, L.M.; Hlaváčová, I.M.; Geryk, V.; Plančár, Š. Investigation of the taper of kerfs cut in steels by AWJ. *Int. J. Adv. Manuf. Technol.* **2015**. [[CrossRef](#)]
 28. Ahmed, D.H.; Naser, J.; Deam, R.T. Particles impact characteristics on cutting surface during the abrasive water jet machining: Numerical study. *J. Mater. Process. Technol.* **2016**, *232*, 116–130. [[CrossRef](#)]
 29. Huang, L.; Folkes, J.; Kinnell, P.; Shipway, P.H. Mechanisms of damage initiation in a titanium alloy subjected to water droplet impact during ultra-high pressure plain waterjet erosion. *J. Mater. Process. Technol.* **2012**, *212*, 1906–1915. [[CrossRef](#)]
 30. Mital, G.; Gajdoš, I.; Ruzbarsky, J.; Jachowicz, T.; Majewski, Ł. Influence and Optimization of the Setting of Input Parameters of Laser Profilometry by the Surface Measurement Manufactured by the AWJ Technology. *Adv. Sci. Technol. Res. J.* **2018**. [[CrossRef](#)]
 31. Wei, X.; Zhu, D.; Ling, X.; Yu, L.; Dai, M. Influence of wet micro-shot peening on surface properties and corrosion resistance of AISI 304 stainless steel. *Int. J. Electrochem. Sci.* **2018**, *13*, 4198–4207. [[CrossRef](#)]
 32. Kretschmer, M.; Aust, E. Recycling of abrasives and process water in the abrasive water jet technique. *Chem. Eng. Technol.* **1999**, *22*, 927–931. [[CrossRef](#)]
 33. Papini, M.; Spelt, J.K. Organic coating removal by particle impact. *Wear* **1997**, *213*, 185–199. [[CrossRef](#)]